

RSC Advances



This is an *Accepted Manuscript*, which has been through the Royal Society of Chemistry peer review process and has been accepted for publication.

Accepted Manuscripts are published online shortly after acceptance, before technical editing, formatting and proof reading. Using this free service, authors can make their results available to the community, in citable form, before we publish the edited article. This *Accepted Manuscript* will be replaced by the edited, formatted and paginated article as soon as this is available.

You can find more information about *Accepted Manuscripts* in the [Information for Authors](#).

Please note that technical editing may introduce minor changes to the text and/or graphics, which may alter content. The journal's standard [Terms & Conditions](#) and the [Ethical guidelines](#) still apply. In no event shall the Royal Society of Chemistry be held responsible for any errors or omissions in this *Accepted Manuscript* or any consequences arising from the use of any information it contains.

A remarkable sensitivity enhancement in gold nanoparticles based lateral flow immunoassay for the detection of *Escherichia coli* O157:H7

Cite this: DOI: 10.1039/x0xx00000x

Xi Cui,^{a, b} Youju Huang,^{*b} Jingyun Wang,^{a, b} Lei Zhang,^b Yun Rong,^b Weihua Lai^{*a} and Tao Chen^{*b}

Received 00th January 2012,
Accepted 00th January 2012

DOI: 10.1039/x0xx00000x

www.rsc.org/

Due to the distinctive features of ease-of-use, low-cost and portable detection, gold nanoparticles (AuNPs) based lateral flow immunoassay (LFA) is an effective and currently used method for the detection of *Escherichia coli* O157:H7 (*E. coli* O157:H7), however, its low sensitivity limits its practical wide-of-use. In our present study, we have systematically optimized the size and uniformity of AuNPs to maximally amplify both visual inspection signals (the color of test line) and quantitative data (light intensity) recorded by 'Assay Reader' instrument. The remarkable enhancement of detection sensitivity can be achieved to 10^2 colony-forming units (CFU)/mL by taking advantages of the optimized AuNPs and the separated incubation of AuNPs/antibody/*E. coli* O157:H7 complex. Quantitative detection of *E. coli* O157:H7 was obtained partially in a wide concentration range with good repeatability. The optimized newly AuNPs-based LFA is well suited for fast quantitative and qualitative food analysis.

1. Introduction

Since its discovery in 1982, *Escherichia coli* O157:H7 (*E. coli* O157:H7) has become a public health concern worldwide because of its strong capability of contaminating food and water, causing severe intestinal infection in humans such as gastrointestinal illness, hemolytic uremic syndrome, and occasionally kidney failure. The great demand for a rapid, accurate and widely-used sensor is an urgent and challenging task for food safety. In the past several decades, numerous efforts have been devoted to various methods for the detection of *E. coli* O157:H7, including molecular biological method (polymerase chain reaction (PCR)-based analysis),¹ DNA and RNA probes,² surface plasmon resonance (SPR),³ immunomagnetic separation (ISM) analysis,⁴ electrochemical biosensor,⁵ and quartz crystal microbalance techniques.⁶ Although each approach has its own advantages, most reports are usually time-consuming, and/or requires expensive equipments and skilled workers.

From the standpoint of ease/wide-of-use, low-cost and portable detection, lateral flow immunoassay (LFA), particularly, gold nanoparticles (AuNPs) based LFA is an effective and currently used method,^{7, 8} which is ideally suitable for on-site testing. Wang and coworkers⁹ have reported a bare-eye-based LFA by using AuNPs for simultaneous detection of three pesticides. Merkoci and co-workers¹⁰ have reported the enhanced LFA using AuNPs loaded with enzymes

to detect the human IgG. This inspired us to establish a special AuNPs-based LFA to detect *E. coli* O157:H7,⁸ but the sensitivity (10^4 CFU/mL) is not very high and limits its practical wide-of-use as a commercial product. The objective of the present study was to develop a high performance AuNPs-based LFA for *E. coli* O157:H7 detection that could achieve high sensitivity and stability.

Generally, there are three ways to improve the detection sensitivity of AuNPs-based LFA such as designing sensitive reader instrument, optimizing test procedure and improving the properties of probe materials.¹¹ Compared with other two ways, exploring the optimized label probes for LFA is a simple and effective mean to improve the detection sensitivity. It is well-known that AuNPs play the critical role in LFA, since both visual inspection signals (the color of test line) and quantitative data (light intensity) recorded by 'Assay Reader' originate from AuNPs, which mainly dependent on their size, shapes, uniformity and aggregation behaviours,¹²⁻²⁷ as well as the wavelength coupling between light source and AuNPs.

In our present study, the size and uniformity of AuNPs were systematically optimized to maximally amplify the detection signals for improving the sensitivity. In addition, the separated incubation of AuNPs/antibody/*E. coli* O157:H7 complex was used to modify the conventional AuNPs-based LFA to improve the stability. The optimized newly AuNPs-based LFA allowed us to detect *E. coli* O157:H7 with an estimated detection limit of 10^2 colony-forming

units (CFU)/mL, which is much lower (two orders in concentration) than that of conventional AuNPs-based LFA.

2. Experimental Section

2.1. Reagents

Hydrogen tetrachloroaurate (III) trihydrate ($\text{HAuCl}_4 \cdot 3\text{H}_2\text{O}$), sodium citrate ($\text{C}_6\text{H}_5\text{Na}_3\text{O}_7 \cdot 2\text{H}_2\text{O}$), bovine serum albumin (BSA), were purchased from Sigma-Aldrich Chemical Co. (St. Louis, MO). Sample pad, nitrocellulose membrane, conjugate release pad, and absorbent pad were obtained from Schleicher and Schuell GmbH (Dassel, Germany). The antibody pairs, namely, murine anti-*E. coli* O157:H7 monoclonal antibody and goat anti-*E. coli* O157:H7 polyclonal antibody and donkey anti-mouse IgG were purchased from Meridian Life Science, Inc (Memphis, TN, USA). Other reagents were of analytical grade and purchased from Sinopharm Chemical Corp. (Shanghai, China).

2.2. Instruments

SkanFlexiBioAssay Reader Systems for the detection of AuNPs-based LFA strip was supplied by Skannex Biotech Co., Ltd (Oslo, Norway). The BioDot XYZ platform combined with a motioncontroller, BioJet Quanti3000k dispenser and AirJetQuanti3000k dispenser for solution dispensing was purchased from BioDot (Irvine, CA). The structures of the nanoparticle were observed by transmission electron microscopy (TEM) conducted on the JEOL JEM 2010 electron microscope. UV-Vis absorption spectra were recorded by virtue of TU-1810 UV/Vis spectrophotometer from Purkinje General Instrument Co. Ltd, Beijing.

2.3. Bacterial strains and growth condition

Bacterial strains were prepared according to our previous report.⁸ *E. coli* O157:H7 strain ATCC 43888 was cultured in Luria-Bertani medium (LB, Oxoid, Basing-stoke, UK) at 37 °C for 20 h before use. Serial dilutions of cultures in phosphate-buffered saline (PBS, Sigma Chemical Company, St. Louis, MO, 0.01 M, pH 7.4) were made and plated onto trypticase soy agar (TSA; Becton, Dickinson and Company, Sparks, MD) to determine the number of viable *E. coli* O157:H7 cells. The plates were then incubated at 37 °C for 24 h. The number was counted when the bacterial colonies could be seen clearly in the plates.

2.4. Preparation of AuNPs with different sizes

AuNPs was prepared according to our previous report.^{26, 28} Briefly, 100 mL of 2.5×10^{-4} M HAuCl_4 solution was heated to 120 °C in an oil bath under vigorous stirring for 30 min. Then, predetermined volume of 1% sodium citrate solution was added into the above solution with continued boiling. After 20 min, the color of the boiled solution changed to ruby red, indicating the formation of AuNPs. The solution was cooled to room temperature for further experiments. Different predetermined volume of sodium citrate solution would lead to different sized AuNPs.

2.5. Preparation of AuNPs with different polydispersity index (PDI)

AuNPs solutions with different PDI were prepared by mixing two AuNPs samples with the pre-widened PDI. The AuNPs with PDI of 0.20 was prepared by the above mentioned Frens method. The other

sample with PDI of 0.65 was prepared as below: 1 mL of 1% sodium citrate solution was added into 100 mL of 2.5×10^{-4} M boiled HAuCl_4 solution heated by electric heating-jacket. A series of AuNPs with the same plasmonic wavelength peak and different PDI such as 0.26, 0.39, 0.47, 0.52, and 0.61 were prepared by adjusting the amount ratio of two AuNPs samples with pre-widened PDI.

2.6. Preparation of AuNPs-antibody complex

300 μL of anti-*E. coli* O157:H7 monoclonal antibody with a concentration of 166 $\mu\text{g}/\text{mL}$ was added into 3 mL of pH-adjusted AuNPs solution and was stirred for 60 min. Then, 0.15 mL of 3% (w/v) BSA solution was added and stirred for another 30 min. Later, 0.15 mL of 10% (w/v) PEG20000 solution was added and stirred for another 30 min. The mixture was centrifuged at 9000 g for 30 min and the precipitate was further dissolved in 300 μL of 50 mM Tris/HCl buffer. The AuNPs-labeled monoclonal antibody complex was dried for 2 h at 30 °C for further use.

2.7. Preparation of AuNPs test strips

The sample pad was pre-treated with 50 mM of borate buffer (pH = 7.4) containing 1% BSA, 0.5% Tween-20, and 0.05% sodium azide, and further dried at 60 °C for 2 h. The goat anti-*E. coli* O157:H7 polyclonal antibody (1.0 mg/ml) and donkey anti-mouse IgG (1.0 mg/ml) were sprayed to the test (T) and control (C) lines on the nitrocellulose membrane, respectively, and dried at 35 °C. The nitrocellulose membrane was blocked with 5% BSA in 0.02 M PBS (pH=7.2) for avoiding the background in the strip. Absorption pad and glass fibre membrane were used without further treatment. The nitrocellulose membrane, absorption pad, glass fibre membrane, and pre-treated sample pad were assembled on the PVC plate to form the final test strip.

2.8. Detection of *E. coli* O157:H7

The *E. coli* O157:H7 culture was diluted into different concentrations from 2.8×10^7 to 2.8×10^2 CFU/mL in sterile PBS, which were further mixed with AuNPs-antibody complex. Then, the mixtures were transmitted onto the test strip. The SkanFlexiBioAssay Reader was used to quantitatively detect the *E. coli* O157:H7 after 10 min. All experiments were performed in triplicate.

3. Results and discussion

Fig.1 shows the schematic of conventional and modified AuNPs-based LFA strips. Generally, the strip mainly contains three parts such as sample pad, nitrocellulose membrane (NC), and absorbent pad (AuNPs-antibody conjugate pad, T and C line with modified corresponding antibodies). In the conventional strip (Fig.1A), the target analysts (*E. coli* O157:H7 culture) flow laterally through the test strip. Firstly they interact with antibody-labelled AuNPs in conjugate pad, and aggregate subsequently at the test line (T line) due to the specific interaction between analyt and antibody, which leads to color-darkening of T line for optical detection. The non-*E. coli* O157:H7 cannot interact with antibody-labelled AuNPs and no red line develops at the test line. The colored antibody-labelled AuNPs should bind to the C line and form a red-colored band regardless of the presence of *E. coli* O157:H7.

Unlike the conventional strip, we proposed the separated incubation of the target analytsts to modify the strip (Fig.1B), which makes LFA displaying three distinctive advantages. Firstly, it eliminates AuNPs-antibody conjugate pad, facilitating the fabrication of the strip. Secondly, the separated incubation of *E. coli* O157:H7 allow us easily control the reaction time (about 5 min), resulting in the complete interaction with antibody labelled AuNPs, rather than instantaneous reaction at AuNPs-antibody conjugate pad. This effective incubation of *E. coli* O157:H7 with antibody labelled AuNPs would lead to high detection performance. Lastly, amount of the separated incubation of *E. coli* O157:H7 can be randomly increased, and used in many times for a large quantity of strips, which significantly improve the stability and repeatability.

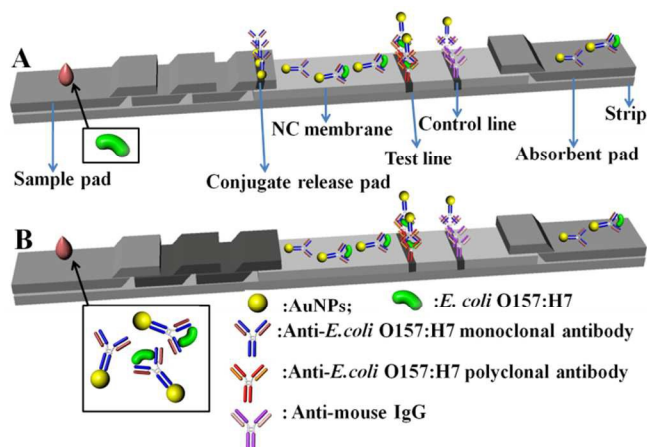


Fig 1. Schematic of conventional (A) and modified (B) AuNPs-based lateral flow immunoassay strips.

It is well known that the size of AuNPs have an important effect on the performance of AuNPs-based LFA.²⁸ Big sized AuNPs usually have high steric hindrance, affecting the interaction with labelled antibody /target analytsts and impeding the fluidity in the strip. While too small sized AuNPs are not the best option to show visual inspection signals. In addition, different labelled antibodies/target analytsts favour the interaction with different size AuNPs. For the detection of *E. coli* O157:H7 in strip, people usually randomly choose AuNPs size in the range from 20 to 60 nm, there is not much report to precisely investigate the small window of size effect on the detection performance.

In order to explore the cut-off size regime where both visual inspection signals and quantitative data (light intensity) could be optimal, we successfully synthesized AuNPs (gold spheres) in a finely tuned small size range from 20 to 54 nm. Fig. 2 shows transmission electron microscopy (TEM) images of AuNPs with various sizes. It is demonstrated that the smallest AuNPs have relatively good shape uniformity, while larger AuNPs are mixed with non-spherical AuNPs, and have a relative broaden size distribution. The average sizes that were obtained from the TEM were 20 ± 1 nm, 28 ± 1 nm, 35 ± 1 nm, 43 ± 2 nm, and 54 ± 3 nm. The UV-vis absorption spectra (Fig 2f) correspond to samples in Fig 2a-e. As the size of AuNPs increases from 20 to 54 nm, the absorption peaks are noticeably red-shifted from 518 to 533 nm,

showing a good agreement with previous reports. The obtained different sized AuNPs were used as labelled probes and testing signal source to investigate the detection efficiency and sensitivity of *E. coli* O157:H7 in LFA.

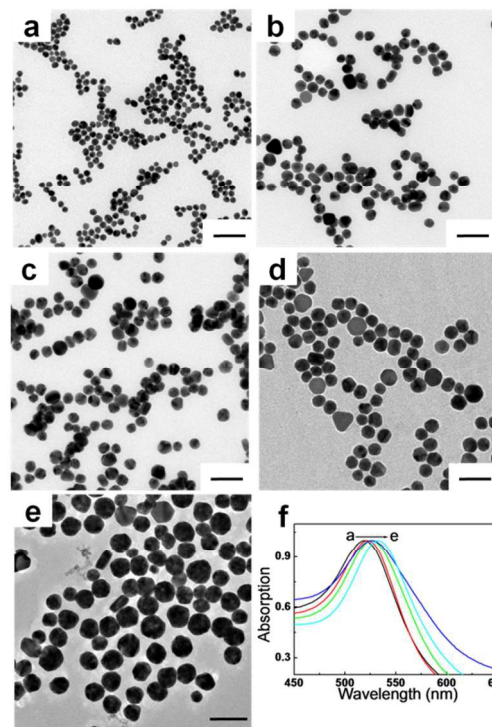


Fig 2. Representative TEM images of AuNPs with different sizes (a: 20 nm; b: 28 nm; c: 35 nm; d: 43 nm; e: 54 nm) and their corresponding UV-vis absorption spectra (f). The scale bar represents 100 nm.

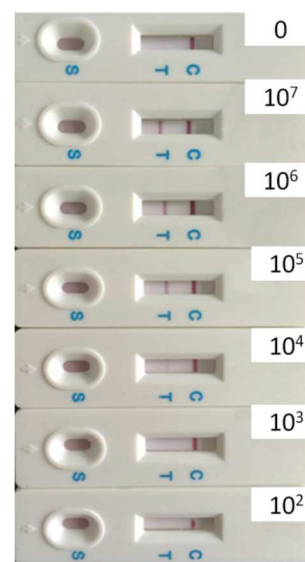


Fig 3. Specificity of strip for the detection of *E. coli* O157:H7 (from 0 to 10^7 CFU/mL) using 35 nm AuNPs.

The different sized AuNPs were first labelled by monoclonal antibody, which interact with *E. coli* O157:H7 and form AuNPs/antibody/*E. coli* O157:H7 complex via the separated incubation. The complex flowed in the strip and was captured by the

goat anti-*E. coli* O157:H7 polyclonal antibody at T line. The visual inspected color and optical intensity at T line can be used to evaluate the detection performances quantitatively and qualitatively, respectively.

Fig. 3 shows a typical batch of AuNPs-based LFA strips to investigate the detection performances of *E. coli* O157:H7 by 35 nm AuNPs-based LFA. The detection procedure was repeated at least three times. In the present study, the visual inspection limit was defined as the minimum analyte concentration required for no obvious visual color on the T line. Following this definition, the visual qualitative inspection limit achieved by 35 nm AuNPs was around 10^3 CFU/mL. The other sized AuNPs labelled LFA samples show the visual qualitative inspection limit 10^3 , 10^4 , 10^5 and 10^6 CFU/mL, corresponding to AuNPs size of 20, 28, 43 and 54 nm, respectively.

In order to precisely, quantitatively study the detection performance of different sized AuNPs probes, the test strips were further subjected to optical density analysis. The light scattering signal of AuNPs aggregates on the T line was monitored by a specific reader. The optical densities of T line under different concentrations of *E. coli* O157:H7 from different sized AuNPs labelled LFTS are recorded and showed in Table 1. Generally, the optical densities were decreased with the decrease of the concentration of *E. coli* O157:H7. Usually, a threshold value was set to determine the detection limits based on the optical density from instrument, which can be roughly calculated from average signal intensity and standard deviation (S.D.) of the negative control (PBS) on T line. The threshold value was the total contribution of average signal intensity and three times of S.D. (average intensity+3S.D.). The corresponding concentration of *E. coli* O157:H7 can be seen as the detection limit, when the detected optical value is bigger than the threshold value. The values highlighted in red color in Table 1 were used to show the detection limit from different sized AuNPs labelled LFTS. The optical density (64 a.u.) on T line from 35 nm AuNPs labelled probe was strong enough to be detected even the concentration of *E. coli* O157:H7 was as low as 10^2 CFU/mL. The same detection process was repeated three times and similar detection limits of 10^2 CFU/mL were obtained, which indicated good reproducibility.

Fig. 4 shows the clear relationship between the size of AuNPs and the detection performances of *E. coli* O157:H7 in LFTS. It is observed that the detection limit from optical density at T line firstly decreases as AuNPs becomes big to 35 nm, and then suddenly increases as the size of AuNPs continuously increases. This finding implies that neither small nor big size of AuNPs benefits the detection limits of *E. coli* O157:H7. The cut-off size is optimized to 35 nm for the best detection performances of *E. coli* O157:H7 in AuNPs-based LFA. As far as steric hindrance and optical property of AuNPs are concerned, smaller sized AuNPs generally have smaller steric hindrance, which provide the strong absorption with antibody and *E. coli* O157:H7, also facilitate the fluidity in the strip. While bigger sized AuNPs in a small size window would offer better optical signals for detection performances. Another possible reason is that the optimized size (35 nm) of AuNPs has a plasmonic

resonance wavelength of 525 nm, as same as the wavelength of light source in 'Assay Reader' instrument. This coupling effect of light wavelength^{29, 30} would maximally amplify the optical property of AuNPs for the detection of *E. coli* O157:H7.

Table 1. The optical density on T line in the detection of *E. coli* O157:H7 (from 0 to 10^7 CFU/mL) using different sized AuNPs.

Concentration (CFU/mL)	Signal intensity of different sized AuNPs based LFA in T line									
	20 nm		28 nm		35 nm		43 nm		54 nm	
	Mean	SD	Mean	SD	Mean	SD	Mean	SD	Mean	SD
PBS	28	1	63	5	37	2	44	5	82	2
2.8×10^7	238	10	208	2	746	32	377	21	202	19
2.8×10^6	413	15	712	23	722	28	865	50	443	39
2.8×10^5	284	8	287	8	872	26	782	31	392	32
2.8×10^4	125	6	132	9	324	31	209	18	110	15
5.6×10^3	101	6	101	5	108	12	126	15	109	12
2.8×10^3	58	5	97	10	121	15	95	11	65	7
5.6×10^2	7	2	90	3	100	7	8	2	32	3
2.8×10^2	10	3	56	6	64	10	32	5	30	5

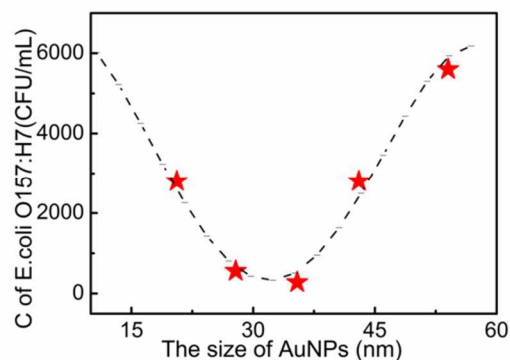


Fig. 4. The relationship between the size of AuNPs and the detection limits of *E. coli* O157:H7. C is the concentration of *E. coli* O157:H7 at the detection limit.

Table 2. The optical density on T line in the detection of *E. coli* O157:H7 (from 0 to 10^7 CFU/mL) using different PDI AuNPs.

Concentration (CFU/mL)	Signal intensity of AuNPs with different PDI based LFA in T line									
	0.26		0.39		0.47		0.52		0.61	
	Mean	SD	Mean	SD	Mean	SD	Mean	SD	Mean	SD
PBS	37	2	55	3	99	2	53	1	60	2
2.8×10^7	746	23	237	15	312	10	148	12	171	12
2.8×10^6	722	26	645	50	566	32	413	22	351	23
2.8×10^5	872	31	242	16	467	41	587	31	127	11
2.8×10^4	324	27	168	20	143	15	128	8	58	10
5.6×10^3	108	12	99	11	73	6	52	3	33	5
2.8×10^3	121	15	69	9	42	5	50	2	34	2
5.6×10^2	100	8	42	10	40	5	16	3	30	3
2.8×10^2	64	9	14	2	33	6	12	3	28	3

The size uniformity of AuNPs was further investigated to evaluate the detection performances of *E. coli* O157:H7 in AuNPs-based LFA. In order to eliminate the light wavelength coupling effect, all samples with different PDI (S-Fig.1f) have the same plasmonic resonance wavelength at 525 nm, which were prepared by artificially mixing the different sized AuNP solution together. The PDI of AuNPs (S-Fig.1a-e) was tuned into 0.26, 0.39, 0.47, 0.52, and 0.61. The optical densities of T line under different concentrations of *E. coli* O157:H7 from different PDI AuNPs labelled LFA are showed in **Table 2**. It is very clear to see the higher PDI lead to the higher detection limit (Fig. 5). We speculate the possible reason as follows: All samples have the same plasmonic resonance wavelength at 525 nm, corresponding to AuNPs with 35 nm, which is the optimized size for the best detection. Sample with the lower PDI should contain more AuNPs with 35 nm, which offer bigger contributions to the detection performance; while the fewer AuNPs with 35 nm in samples with the higher PDI would lead to the worse detection limits. Sample with the lower PDI was much higher uniform than that with higher PDI, which provided the optimized optical signals and smaller steric hindrance for absorption with antibody and *E. coli* O157:H7. These would lead to the best detection performance.

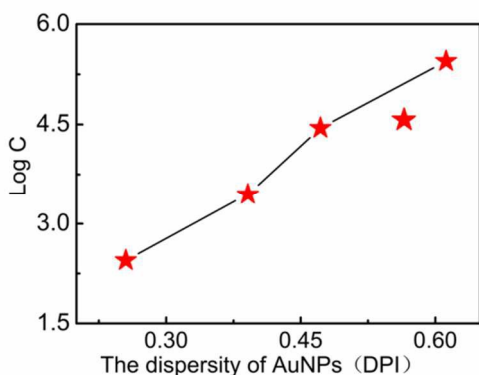


Fig 5. The relationship between the DPI of AuNPs and the detection limits of *E. coli* O157:H7 (C is the concentration of *E. coli* O157:H7).

4. Conclusions

We have shown that a new modified AuNPs-based LFA can remarkably improve the detection performance of *E. coli* O157:H7. Firstly, the separated incubation of *E. coli* O157:H7 and antibody labelled AuNPs significantly improve the stability of strip and repeatability of experimental data. Secondly, a cut-off size of AuNPs in a small size window was found to maximally amplify both visual inspection and optical signals. The optimized newly AuNPs-based LFA would provide much more possibility in fast quantitative and qualitative food analysis.

Acknowledgements

We thank the Chinese Academy of Science for Hundred Talents Program, Chinese Central Government for Thousand Young Talents Program, the Natural Science Foundation of China (21404110, 51473179, 51303195, 21304105), Excellent Youth Foundation of Zhejiang Province of China (LR14B040001), and Ningbo Science

and Technology Bureau (Grant 2014B82010). Earmarked fund for Jiangxi Agriculture Research System (JXARS-03), Jiangxi education bureau technology put into use project (KJLD13009), and the Nanchang Technological Program (2012-CYH-DW-SP-001).

Notes and references

^a State Key Laboratory of Food Science and Technology, Nanchang University, Nanchang 330047, China.

^b Division of Polymer and Composite Materials, Ningbo Institute of Material Technology and Engineering, Chinese Academy of Science, No. 1219 Zhongguan West Road, Zhenhai District, Ningbo 315201, China

1. D. Hardegger, D. Nadal, W. Bossart, M. Altwegg and F. Dutly, *J. Microbiol. Meth.*, 2000, **41**, 45-51.
2. X.-T. Mo, Y.-P. Zhou, H. Lei and L. Deng, *Enzyme Microbiol. Technol.*, 2002, **30**, 583-589.
3. H. Uchida, K. Fujitani, Y. Kawai, H. Kitazawa, A. Horii, K. Shiiba, K. Saito and T. Saito, *Biosci. Biotechnol. Biochem.*, 2004, **68**, 1004-1010.
4. X. Cui, Q.-R. Xiong, Y.-H. Xiong, S. Shan and W.-H. Lai, *Chin J Anal Chem.*, 2013, **41**, 1812-1816.
5. C. M. Pandey, I. Tiwari and G. Sumana, *RSC Adv.*, 2014, **4**, 31047-31055.
6. X. Su, S. Low, J. Kwang, V. H. T. Chew and S. F. Y. Li, *Sens. Actuators B*, 2001, **75**, 29-35.
7. E.-H. Lee, Y. A. Kim, Y. T. Lee, B. D. Hammock and H.-S. Lee, *Food Agric. Immunol.*, 2012, **24**, 129-138.
8. Q.-Y. Xie, Y.-H. Wu, Q.-R. Xiong, H.-Y. Xu, Y.-H. Xiong, K. Liu, Y. Jin and W.-H. Lai, *Biosens. Bioelectron.*, 2014, **54**, 262-265.
9. L. M. Wang, J. Cai, Y. L. Wang, Q. K. Fang, S. Y. Wang, Q. Cheng, D. Du, Y. H. Lin and F. Q. Liu, *Microchim. Acta*, 2014, **181**, 1565-1572.
10. C. Parolo, A. de la Escosura-Muniz and A. Merkoci, *Biosens. Bioelectron.*, 2013, **40**, 412-416.
11. L. Zhang, Y. Huang, J. Wang, Y. Rong, W. Lai, J. Zhang and T. Chen, *Langmuir*, 2015, **In press**. DOI: [10.1021/acs.langmuir.5b00592](https://doi.org/10.1021/acs.langmuir.5b00592).
12. H. Chen, L. Shao, Q. Li and J. Wang, *Chem. Soc. Rev.*, 2013, **42**, 2679-2724.
13. L. M. Liz-Marzan, C. J. Murphy and J. Wang, *Chem. Soc. Rev.*, 2014, **43**, 3820-3822.
14. Y. Huang, A. R. Ferhan, Y. Gao, A. Dandapat and D.-H. Kim, *Nanoscale*, 2014, **6**, 6496-6500.
15. J. Allouche, S. Soule, J.-C. Dupin, S. Masse, T. Coradin and H. Martinez, *RSC Adv.*, 2014, **4**, 63234-63237.
16. E. C. Dreaden, A. M. Alkilany, X. Huang, C. J. Murphy and M. A. El-Sayed, *Chem. Soc. Rev.*, 2012, **41**, 2740-2779.
17. Y. Huang, A. R. Ferhan and D.-H. Kim, *Nanoscale*, 2013, **5**, 7772-7775.
18. C. P. Rao, D. S. Yarramala and S. Doshi, *RSC Adv.*, 2015.
19. Y. Huang and D.-H. Kim, *Nanoscale*, 2011, **3**, 3228-3232.
20. J. Xin, R. Zhang and W. Hou, *RSC Adv.*, 2014, **4**, 5834-5837.
21. S. Eustis and M. A. El-Sayed, *Chem. Soc. Rev.*, 2006, **35**, 209-217.
22. Y. Huang, L. Wu, X. Chen, P. Bai and D.-H. Kim, *Chem. Mater.*, 2013, **25**, 2470-2475.

ARTICLE

Journal Name

23. H. Yuan, K. P. F. Janssen, T. Franklin, G. Lu, L. Su, X. Gu, H. Uji-i, M. B. J. Roeffaers and J. Hofkens, *RSC Adv.*, 2015, **5**, 6829-6833.
24. G. Frens, *Nature Physical Science*, 1973, **241**, 20-22.
25. L. Dykman and N. Khlebtsov, *Chem. Soc. Rev.*, 2012, **41**, 2256-2282.
26. Y. Huang and D.-H. Kim, *Langmuir*, 2011, **27**, 13861-13867.
27. N. Khlebtsov and L. Dykman, *Chem. Soc. Rev.*, 2011, **40**, 1647-1671.
28. L. Zhang, L. Dai, Y. Rong, Z. Liu, D. Tong, Y. Huang and T. Chen, *Langmuir*, 2015, **31**, 1164-1171.
29. H. Su, Y. Zhong, T. Ming, J. Wang and K. S. Wong, *J. Phys. Chem. C*, 2012, **116**, 9259-9264.
30. W. Ni, T. Ambjörnsson, S. P. Apell, H. Chen and J. Wang, *Nano Lett.*, 2010, **10**, 77-84.